

**Xing Xian Yu, Jamie L. Barger, Bert B. Boyer, Martin D. Brand, Guohua Pan and Sean H. Adams**

*Am J Physiol Endocrinol Metab* 279:433-446, 2000.

**You might find this additional information useful...**

---

This article cites 47 articles, 18 of which you can access free at:

<http://ajpendo.physiology.org/cgi/content/full/279/2/E433#BIBL>

This article has been cited by 7 other HighWire hosted articles, the first 5 are:

**Regulation of UCP1 and UCP3 in arctic ground squirrels and relation with mitochondrial proton leak**

J. L. Barger, B. M. Barnes and B. B. Boyer  
*J Appl Physiol*, July 1, 2006; 101 (1): 339-347.

[Abstract] [Full Text] [PDF]

**Enterostatin decreases postprandial pancreatic UCP2 mRNA levels and increases plasma insulin and amylin**

D. Arsenijevic, E. Gallmann, W. Moses, T. Lutz, C. Erlanson-Albertsson and W. Langhans  
*Am J Physiol Endocrinol Metab*, July 1, 2005; 289 (1): E40-E45.

[Abstract] [Full Text] [PDF]

**Effects of Wnt Signaling on Brown Adipocyte Differentiation and Metabolism Mediated by PGC-1{alpha}**

S. Kang, L. Bajnok, K. A. Longo, R. K. Petersen, J. B. Hansen, K. Kristiansen and O. A. MacDougald

*Mol. Cell. Biol.*, February 15, 2005; 25 (4): 1272-1282.

[Abstract] [Full Text] [PDF]

**Expression of uncoupling protein 3 is upregulated in skeletal muscle during sepsis**

X. Sun, C. Wray, X. Tian, P.-O. Hasselgren and J. Lu  
*Am J Physiol Endocrinol Metab*, September 1, 2003; 285 (3): E512-E520.

[Abstract] [Full Text] [PDF]

**Cold elicits the simultaneous induction of fatty acid synthesis and {beta}-oxidation in murine brown adipose tissue: prediction from differential gene expression and confirmation in vivo**

X. X. YU, D. A. LEWIN, W. FORREST and S. H. ADAMS  
*FASEB J*, February 1, 2002; 16 (2): 155-168.

[Abstract] [Full Text] [PDF]

Medline items on this article's topics can be found at <http://highwire.stanford.edu/lists/artbytopic.dtl> on the following topics:

Biochemistry .. Lipopolysaccharides  
Biochemistry .. Uncoupling Protein  
Medicine .. Endotoxins  
Medicine .. Endotoxemia  
Medicine .. Hypothermia  
Physiology .. Mice

Updated information and services including high-resolution figures, can be found at:

<http://ajpendo.physiology.org/cgi/content/full/279/2/E433>

Additional material and information about *AJP - Endocrinology and Metabolism* can be found at:

<http://www.the-aps.org/publications/ajpendo>

---

This information is current as of June 12, 2007 .

# Impact of endotoxin on UCP homolog mRNA abundance, thermoregulation, and mitochondrial proton leak kinetics

XING XIAN YU,<sup>1</sup> JAMIE L. BARGER,<sup>2</sup> BERT B. BOYER,<sup>2</sup>  
MARTIN D. BRAND,<sup>3</sup> GUOHUA PAN,<sup>1</sup> AND SEAN H. ADAMS<sup>1</sup>

<sup>1</sup>Department of Endocrinology, Genentech, Inc., South San Francisco, California 94080;

<sup>2</sup>Institute of Arctic Biology, University of Alaska, Fairbanks, Alaska 99775;

and <sup>3</sup>Medical Research Council Dunn Human Nutrition Unit,  
Cambridge CB2 2XY, United Kingdom

Received 20 December 1999; accepted in final form 16 March 2000

**Yu, Xing Xian, Jamie L. Barger, Bert B. Boyer, Martin D. Brand, Guohua Pan, and Sean H. Adams.** Impact of endotoxin on UCP homolog mRNA abundance, thermoregulation, and mitochondrial proton leak kinetics. *Am J Physiol Endocrinol Metab* 279: E433–E446, 2000.—Linking tissue uncoupling protein (UCP) homolog abundance with functional metabolic outcomes and with expression of putative genetic regulators promises to better clarify UCP homolog physiological function. A murine endotoxemia model characterized by marked alterations in thermoregulation was employed to examine the association between heat production, UCP homolog expression, and mitochondrial proton leak (“uncoupling”). After intraperitoneal lipopolysaccharide (LPS, ~6 mg/kg) injection, colonic temperature ( $T_c$ ) in adult female C57BL/6J mice dropped to a nadir of ~30°C by 8 h, preceded by a four- to fivefold drop in liver UCP2 and UCP5/brain mitochondrial carrier protein 1 mRNA levels, with no change in their hindlimb skeletal muscle (SKM) expression. SKM UCP3 mRNA rose fivefold during development of hypothermia and was correlated with an LPS-induced increase in plasma free fatty acid concentration. UCP2 and UCP5 transcripts recovered about three- to sixfold in both tissues starting at 6–8 h, preceding a recovery of  $T_c$  between 16 and 24 h. SKM UCP3 followed an opposite pattern. Such results are not consistent with an important influence of UCP3 in driving heat production but do not preclude a role for UCP2 or UCP5 in this process. The transcription coactivator PGC-1 displayed a transient LPS-evoked rise (threefold) or drop (two- to fivefold) in SKM and liver expression, respectively. No differences between control and LPS-treated mouse liver or SKM in vitro mitochondrial proton leak were evident at time points corresponding to large differences in UCP homolog expression.

uncoupling proteins; lipopolysaccharide; metabolic rate; hypothermia; peroxisome proliferator-activated receptor

MAINTENANCE OF A STABLE body temperature involves a precise balance between heat acquisition and loss, driven by a complex interaction of physiological, behavioral, and environmental processes. The ability to generate and regulate metabolic heat is a hallmark of endothermy and a critical adjunct to other

events that contribute to efficient thermoregulation (physiological control of convective and conductive heat loss, heat- or cold-seeking behavior, etc.). Heat production in endotherms is in part ascribed to a global energetic inefficiency inherent to cellular biochemical reactions augmented by additional energy-consuming mechanisms, including protein turnover and futile cycling, which drive ATP consumption (9). The relative contribution of these and other mechanisms toward establishment of metabolic rate is the subject of active research. Identification of the molecular and biochemical components underlying regulation of heat balance has important ramifications for the development of pharmaceutical intervention strategies to treat metabolic disorders, and for clarifying regulation of adaptational thermoregulation in nature.

One potential locus of thermoregulatory control is proton flux across the inner mitochondrial membrane. It is now apparent that the inward flow of protons via mechanisms independent of  $F_1F_0$ ATP synthase (termed “proton leak”) is not insignificant and would act to dissipate fuel-derived energy as heat (9, 37). In rodents, this process is modified by changes in thyroid status (18, 24) and in some forms of obesity (11), and it may account for ~20 to 40% of tissue metabolic rate under normal conditions (9). The underpinnings of proton leak remain to be established. The characterization and cloning of UCP1 (8, 19), a specific uncoupling protein (UCP) that facilitates accelerated proton leak in stimulated rodent brown adipose tissue (BAT), have supported the notion that bodywide proton leak may be regulated by specific mitochondrial proteins. Recent descriptions of putative UCP homologs residing in various tissues (7, 15–17, 28, 40, 42, 46) have sparked interest in exploring whether these proteins influence tissue-specific or whole animal heat production. Some studies examining homolog mRNA abundance

Address for reprint requests and other correspondence: S. H. Adams, Dept. of Endocrinology, Genentech, Inc., 1 DNA Way, South San Francisco, CA 94080 (E-mail: shadams@gene.com).

The costs of publication of this article were defrayed in part by the payment of page charges. The article must therefore be hereby marked “advertisement” in accordance with 18 U.S.C. Section 1734 solely to indicate this fact.

are consistent with a role for UCP homologs in modifying proton leak and metabolic rate, whereas other results may point to additional metabolic roles for these proteins.

Supportive of an uncoupling role for UCP homologs, there are certain conditions in which UCP2 or UCP3 mRNAs appear to correlate with *in vitro* determinations of mitochondrial proton leak (11, 24). Furthermore, expression of UCP2 and UCP3 in rodent BAT rises in response to cold exposure (4), concurrent with increased proton leak in this tissue. Thyroid hormone administration to rodents, a condition in which tissue proton leak has been shown to rise (18, 24), increases UCP3 mRNA in muscle (17, 21, 24) and upregulates UCP2 in a tissue-specific manner (21, 25). UCP5 [also termed brain mitochondrial carrier protein 1 (BMCP1) (40)] is widely expressed, and its liver mRNA level is altered in parallel with metabolism during fasting, cold challenge, and a high-fat diet in obesity-resistant mice; cold also induces its expression in the brain (46). Brain-specific UCP4 mRNA is upregulated in this organ upon exposure of mice to cold (46), consistent with the hypothesis that UCP4 could be involved in localized adaptational thermoregulation (27). Results that do not support a classic thermogenic uncoupling role for UCP2 and UCP3 include reports of a rise in their skeletal muscle (SKM) transcript levels during fasting or food restriction (5, 6, 9a, 17, 20, 31, 32, 38, 44), despite a lack of change in *in vitro* SKM proton leak (9a), the higher abundance of UCP2 mRNA sometimes observed in obesity (11, 16, 31), and the lack of a consistent demonstration for a robust rise in SKM mRNAs upon cold exposure (6, 7, 15; but see also Ref. 5 for induction of UCP2 by cold).

Divergent tissue expression patterns (UCP2 is widely expressed, whereas UCP3 is most abundant in SKM and BAT, but without expression in liver) and differential modification after certain experimental manipulations (17, 44, 45) indicate that some differences in gene regulation exist when UCP2 and UCP3 are compared. Often, however, patterns of expression for these homologs converge (4). The association between their expression and that of UCP5 and the differential expression of UCP5 in SKM have not been reported.

Animal models that display broad alterations in heat production serve as valuable tools to better understand cellular mechanisms that drive metabolic rate, including the role of UCP homologs. The murine model of endotoxemia provides an interesting system in this regard, because administration of lipopolysaccharide (LPS) elicits a range of thermoregulatory responses, including acute hypothermia usually followed by temperature recovery (23, 33). It is plausible that LPS-induced changes in UCP homolog expression and uncoupling activity in metabolically relevant tissues underlie the decline and/or rebound of body temperature in this model. Indeed, it has been reported that liver UCP2 mRNA is increased at 12–24 h after LPS administration in rodents (11, 12, 14), leading to speculation that this rise may signal an increase in active

uncoupling and thermogenesis in that organ (14). However, no physiological or biochemical correlates were presented, and studies investigating the temporal effects of LPS on UCP homolog expression in SKM have not been reported. In this study, we examined the degree to which UCP homolog mRNA abundance correlates with observed changes in functional metabolic outcomes (body temperature, mitochondrial proton leak, and metabolic rate) after a hypothermia-inducing dose of LPS, focusing on the liver and SKM, which are estimated to contribute over one-half of the metabolic rate under normal conditions (9). In an effort to better understand the regulatory factors driving observed UCP homolog expression changes, the association between such changes with those of the recently characterized peroxisome proliferator-activated receptor- $\gamma$  (PPAR $\gamma$ ) coactivator 1 [PGC-1 (34, 45)] was assessed. PGC-1 has been implicated in the induction of genes encoding UCP1, UCP2, and other metabolically relevant proteins (34, 45). In addition, the idea was explored that core body temperature-sensing pathways trigger alterations in UCP homolog gene expression in LPS-treated mice. Despite large changes in liver and SKM UCP homolog mRNA abundance, PGC-1 expression, and evidence for remarkable metabolic shifts after LPS, no association of these parameters with mitochondrial proton leak could be discerned. A disconnect between PGC-1 and UCP2 expression (particularly evident in SKM) after LPS indicated that under these conditions regulatory factors distinct from PGC-1 modulated UCP2 transcription.

## MATERIALS AND METHODS

**Animals.** All animal studies conformed to the “Guiding Principles for Research Involving Animals and Human Beings” and were done in accordance with guidelines set forth by the Institutional Animal Care and Use Committee at Genentech. Female C57BL6/J mice (Jackson Labs, Bar Harbor, ME) aged 54–63 days and weighing 16–18 g were used for all studies. Mice were received 1 wk before experimentation and, unless otherwise noted, were housed on a 12:12-h light-dark cycle (lights on at 0600) at 22°C and were fed normal rodent chow (Ralston Purina Chow 5010, St. Louis, MO). Where indicated, heparinized blood was obtained by heart puncture from CO<sub>2</sub>-anesthetized mice and was promptly centrifuged to obtain plasma, after which free fatty acid (FFA) concentrations were measured (NEFA C kit, Wako Chemicals, Richmond, VA).

**Reagents.** LPS was a Westphal preparation from *Escherichia coli* 055:B5 (Lot 121379JD, Difco Laboratories, Detroit, MI). Methyltriphenylphosphonium bromide (TPMP) was purchased from Aldrich Chemicals (Milwaukee, WI). Collagenase Type IV was obtained from Worthington Biochemical (Lakewood, NJ). Other chemicals were from Sigma (St. Louis, MO).

**LPS administration.** To best compare results with those reported by Faggioni et al. (14), conditions used herein were generally similar to those used by that group. A working stock of LPS was prepared in sterile PBS, and aliquots were frozen at –20°C and thawed once on the day of the experiment. For all LPS experiments, LPS was injected intraperitoneally at 100  $\mu$ g/mouse (5.6–6.2 mg/kg) in a volume of 100  $\mu$ l between 1430 and 1630. Preliminary experiments indi-

cated that this dosage elicited a marked hypothermia compared with doses 10- to 100-fold lower (not shown) and was similar in magnitude to the amount given by Faggioni et al. Control mice received 100  $\mu$ l PBS intraperitoneally. After injection, mice were given access to water but were fasted to account for the effects of LPS-induced cachexia (14). Various parameters hypothesized to be influenced by endotoxemia were monitored for up to 48 h (see below). Unless otherwise noted (see *study 2*), mice were housed at 22°C for the duration of each experiment.

**Body temperature and UCP homolog mRNA after LPS (studies 1 and 2).** An initial experiment (*study 1*) was designed to ascertain whether mRNAs encoding UCP homologs track metabolism after LPS. At intervals of 0, 2, 4, 6, 8, 16, 24, and 48 h after injection, body temperatures in groups of control or LPS-treated mice ( $n = 3-5$  per treatment per time point) were determined as follows. Mice were removed from the cage with minimal disturbance, and colonic temperature ( $T_c$ ) was rapidly measured with a mouse rectal thermocouple (Physitemp BAT-10 recorder/RET-3 thermocouple, Clifton, NJ). Mice were then killed under  $CO_2$ , and tissues were harvested and snap-frozen. For studies of SKM, whole hindlimb SKM was excised, and visible fat and nervous tissue were removed before freezing. In *study 2*, a new group of mice were subjected to the same protocol but were placed in a warm (34°C) room after injection to test the effects of core temperature maintenance on LPS-altered parameters.

Total RNA preparations from liver or pulverized SKM of individual mice were made (Ultraspec reagent, Biotecx Laboratories, Houston, TX) and were assayed for mRNA abundance with quantitative real time RT-PCR after digestion of samples with DNase per manufacturer's instructions (GIBCO BRL, Grand Island, NY). This system employed primers and probes specific to murine UCP2, total UCP5, UCP3, PGC-1, and macrophage-specific marker F4/80 (Table 1). 18S primers/probes were purchased from Perkin-Elmer Applied Biosystems (Foster City, CA). Specificity of UCP primers/probes was confirmed by testing against a panel of plasmids containing cDNAs encoding UCPS 2-5, and the amount of RNA analyzed was in the linear range of the assay (not shown). Reactions and detection were carried out with the use of a model 7700 sequence detector and TaqMan reagents (PE Applied Biosystems) in a volume of 50  $\mu$ l and containing 100 ng RNA, 3 mM  $MgCl_2$ , reaction buffer A (1 $\times$ ), 12.5 U MuLV reverse transcriptase, 1.25 U TaqGold, forward and reverse primers (0.01 OD each), and 0.1  $\mu$ M probe (18S analyses utilized 240 pg RNA, 5.5 mM  $MgCl_2$ , and 0.05  $\mu$ M probe/primer). Cycling conditions were 50°C for 15 min and 95°C for 10 min, followed by 40 cycles of 95°C for 15 s and 60°C for 1 min. Putative housekeeping gene mRNAs ( $\beta$ -actin, GAPDH, RPL19) tested in a subset of LPS liver samples indicated that their levels declined over time after injection (14); thus 18S mRNA abundance was used as a loading control, and all values reported herein represent 18S-corrected values. Based on established tissue distribution pat-

terns for the UCP homologs (see the introductory section of this paper), analyses focused on UCP3 in SKM and UCP2/UCP5 in SKM and liver.

**Mitochondrial proton leak measurements (study 3).** In *study 3*, examining the correlation between UCP homolog mRNA and mitochondrial proton leak in liver and SKM, a new set of mice was used (injection protocol identical to that of *study 1*). At certain times after injection, mitochondria were prepared from control or LPS-injected animals and assayed in parallel. Protocols for mitochondria isolation and measurement of proton leak were patterned after those reported elsewhere (37). After measuring  $T_c$ , mice were killed under  $CO_2$ , livers were removed, a fraction was snap-frozen for mRNA analysis, and the remainder was placed in ice-cold STE buffer (250 mM sucrose, 5 mM Tris, 2 mM EGTA, pH 7.4). For mitochondria, livers from 3-5 mice per treatment were pooled and minced on ice in a small volume of STE. Samples were then processed by standard homogenization and centrifugation methods (37), with the final mitochondrial pellet resuspended in 500  $\mu$ l STE and kept on ice until analysis. Hindlimb SKM was obtained from a separate set of mice. For these studies, muscle from a single mouse per treatment was obtained and snap-frozen for RNA, after which hindlimb muscles from each of 5-6 mice per treatment were pooled to obtain mitochondria. Samples were processed by use of a slight modification of the protocols employed by Rolfe et al. (37): after removal of visible fat and nervous tissue, samples in the current study were placed in ice-cold CP1 buffer (100 mM KCl, 50 mM Tris  $\cdot$  HCl, 2 mM EGTA, pH 7.4), minced on an ice-cold glass plate, and added to 50 ml of pH 7.4 CP2 buffer (100 mM KCl, 50 mM Tris  $\cdot$  HCl, 2 mM EGTA, 0.5% FFA-free BSA, 5 mM  $MgCl_2$ , 1 mM ATP, 2.1 U/ml nagarse; ATP/nagarse added on day of experiment). Samples were kept on ice for 10 min with occasional agitation and then subjected to a brief (10 s, 20,000 rpm) polytron on ice (PowerGen 700, Fisher Scientific, Santa Clara, CA) and an additional 10-min cold incubation before differential centrifugation and washes at 4°C (37). Supernatants from the initial 10-min/500-g centrifugation were poured through two layers of gauze before the high-speed spins/washes. Resulting pellets were resuspended in 200-300  $\mu$ l CP1 and kept on ice until assay. Mitochondria prepared in this way yielded respiratory control ratios (state 3/state 4 respiration with succinate as substrate) of >5 (liver) or >3 (SKM). Protein concentrations were determined by the bicinchoninic acid assay (BCA kit, Pierce, Rockford IL).

For proton leak assays, mitochondria were introduced at ~1 mg protein/ml to a water-jacketed chamber containing 3.5 ml pH 7.2 KHE buffer (120 mM KCl, 5 mM  $KH_2PO_4$ , 3 mM HEPES, 1 mM EGTA, 0.3% fatty acid-free BSA) containing rotenone (5  $\mu$ M), oligomycin (1  $\mu$ g/ml), and nigericin (80 ng/ml). Oxygen consumption ( $\dot{V}O_2$ ) of mitochondria was monitored by a Clark-type model 300 oxygen electrode/Type 1 electronic stirring head (Rank Brothers, Cambridge, UK) interfaced with a Unit DW4 oxygen back-

Table 1. Murine-specific primer/probe sequences used for real time RT-PCR analyses

Gene	Forward Primer	Probe	Reverse Primer
UCP2	TACCAGAGCACTGTCGAAGCC	ACAAGACCATTGCACGAGAGGAAGGGAT	AGTCCCTTTCCAGAGGCC
UCP3	AGAGGGTGGCTCAGGAGGG	CCCACGGCCTTCTACAAAGGATTTGTG	CCCAGACGCAGAAAGGAGG
UCP5	GGGTGTGGTCCCAACTGCT	CGTGCTGCAATCGTTGTGGGAGTAGAG	TTCTTGGTAATATCATAAACGGGCA
PGC-1	GTAGGCCAGGTACGACAGC	TGAAGCCTATGAGCACGAAAGGCTCAA	GCTCTTTGCGGTATTTCATCCC
F4/80	TCTGAGGCAGAAGCTCTGCA	AGAAGTCTCTAACTCAAGGACACGAGGTTGCTG	ATCTGGCAATGGCCTTGA

UCP, uncoupling protein; PGC-1, peroxisome proliferator-activated receptor- $\gamma$  coactivator 1; F4/80, a macrophage-specific marker. Sequences are 5' to 3'; probes were labeled with 5' FAM/3' TAMRA.

off system (Gritech Engineering, UK) and a chart recorder (Kipp and Zonen). Oxygen saturation values of 471 nmol O/ml and 406 nmol O/ml were used to calculate  $\dot{V}O_2$  of preparations assayed at 26 and 37°C, respectively (35). Measurements of mitochondrial TPMP<sup>+</sup> uptake were made with a TPMP<sup>+</sup>-sensitive electrode (37) referenced with a semimicro CE2 pH electrode (Unicam, Cambridge, UK) and interfaced with a back-off box, pH meter, and

chart recorder. Within each individual run, a standard curve of recorder distance vs. [TPMP<sup>+</sup>] was calculated using 1- $\mu$ M additions of TPMP<sup>+</sup> to 5  $\mu$ M (liver) or 0.5- $\mu$ M additions to 2  $\mu$ M (SKM). After addition of Na<sub>2</sub>-succinate (4 mM), respiration was titrated by additions of Na<sub>2</sub>-malonate ( $\leq 7.9$   $\mu$ M and 4.5  $\mu$ M in liver and SKM, respectively). Drift was determined by addition of 2  $\mu$ M carbonyl cyanide *p*-(trifluoromethoxy)phenylhydrazone to abolish membrane potential at the end of each assay run. Mitochondrial membrane potential ( $\Delta\psi$ , in mV) was calculated with the equation

$$\Delta\psi = 61.5 \log \{ ([TPMP] \text{ added} - \text{external } [TPMP]) \times TPMP \text{ binding correction} / (0.001 \times \text{mg mito protein/ml} \times \text{external } [TPMP]) \}$$

where the TPMP binding corrections are 0.4 and 0.35 for liver and SKM, respectively (37).

**Hepatocyte isolation (study 4).** Changes in UCP homolog and PGC-1 expression in hepatocytes isolated from control and LPS-treated mice (injection protocols identical to that in *study 1*) were assessed with the following procedure. At certain times after injection, mice were anesthetized by intraperitoneal injection of 100  $\mu$ l ketamine-xylazine-saline (2:1:10) and immobilized, and the inferior vena cava was exposed. With introduction of air bubbles avoided at all steps, a 22-gauge Angiocath catheter (Becton-Dickinson, Rutherford, NJ) was placed below the liver, with clotting avoided by injection of 200  $\mu$ l 1,000 U/ml heparin. An infusion line containing 37°C *buffer I* (142 mM NaCl, 6.7 mM KCl, 100 mM HEPES, 5.3 mM EGTA, pH 7.4) was attached, flow was initiated at 4 ml/min, the portal vein was severed, and the inferior vena cava below the heart was ligated. After 5 min, flow was switched to 37°C *buffer II* (66.7 mM NaCl, 6.7 mM KCl, 100 mM HEPES, 4.8 mM CaCl<sub>2</sub>, 1% FFA-free BSA, 77 U/ml Type IV collagenase, pH 7.6) for 20–30 min. Perfused livers were excised, the gall bladder was removed, and cells were dissociated by cutting the liver capsule and agitating the tissue in a small volume of *buffer II* with mincing. The preparation was poured into a 50-ml conical tube through a 250  $\mu$ m filter and then a 40  $\mu$ m filter. The preparation was brought to  $\sim 20$  ml with cold HBSS and then centrifuged at  $\sim 50 g$  for 3 min. The supernatant containing nonparenchymal cells (NPCs) with nonpelleted hepatocytes was withdrawn and saved on ice (cells in supernatants from this and subsequent washes are termed the “NPC-enriched fraction”). Cells were resuspended in 20 ml cold HBSS via gentle rocking and recentrifuged at 50  $g$  for 1 min, and the supernatant was withdrawn. This step was repeated, and the resulting

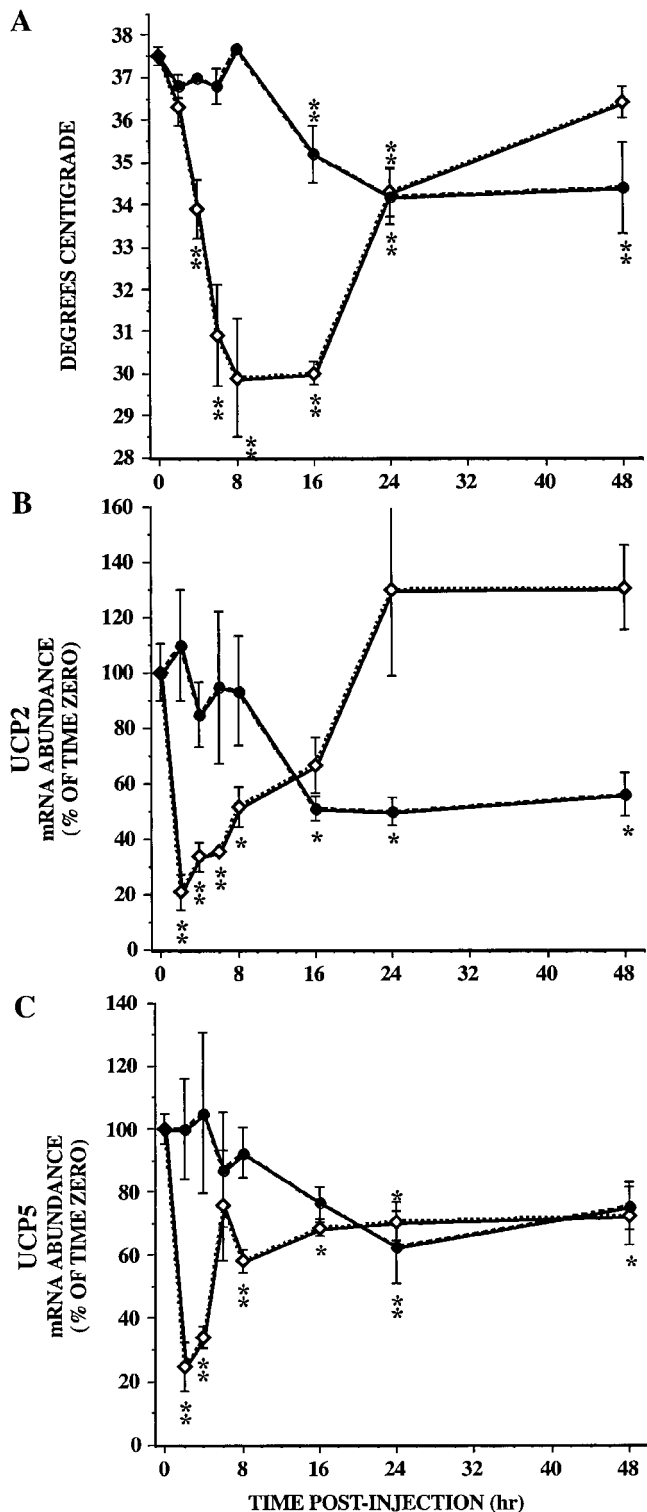


Fig. 1. Marked hypothermia and large changes in whole liver uncoupling protein (UCP) homolog mRNA abundance in mice treated with lipopolysaccharide (LPS). Adult female C57BL/6J mice were treated with a single ip dose of PBS (controls, ●) or LPS ( $\sim 6$  mg/kg, ◇), after which colonic temperature (A), whole liver UCP2 mRNA abundance (B), and whole liver UCP5 mRNA abundance (C) were determined over 48 h postinjection (*study 1*, see MATERIALS AND METHODS). Animals were injected (0 h) between 1530 and 1630, fasted after treatment, and housed at 22°C for the duration of the study (see MATERIALS AND METHODS for details). Each point represents the mean  $\pm$  SE of 3–5 independent measurements (\* $P \leq 0.05$ , \*\* $P \leq 0.01$  vs. *time 0* values); some error bars are within the symbol. Not indicated are significant differences ( $P < 0.05$ ) between LPS mice and time-matched controls, occurring at 4–8, 16, and 48 h (temperature), 2–6, 24, and 48 h (UCP2), and 2, 4, and 8 h (UCP5).

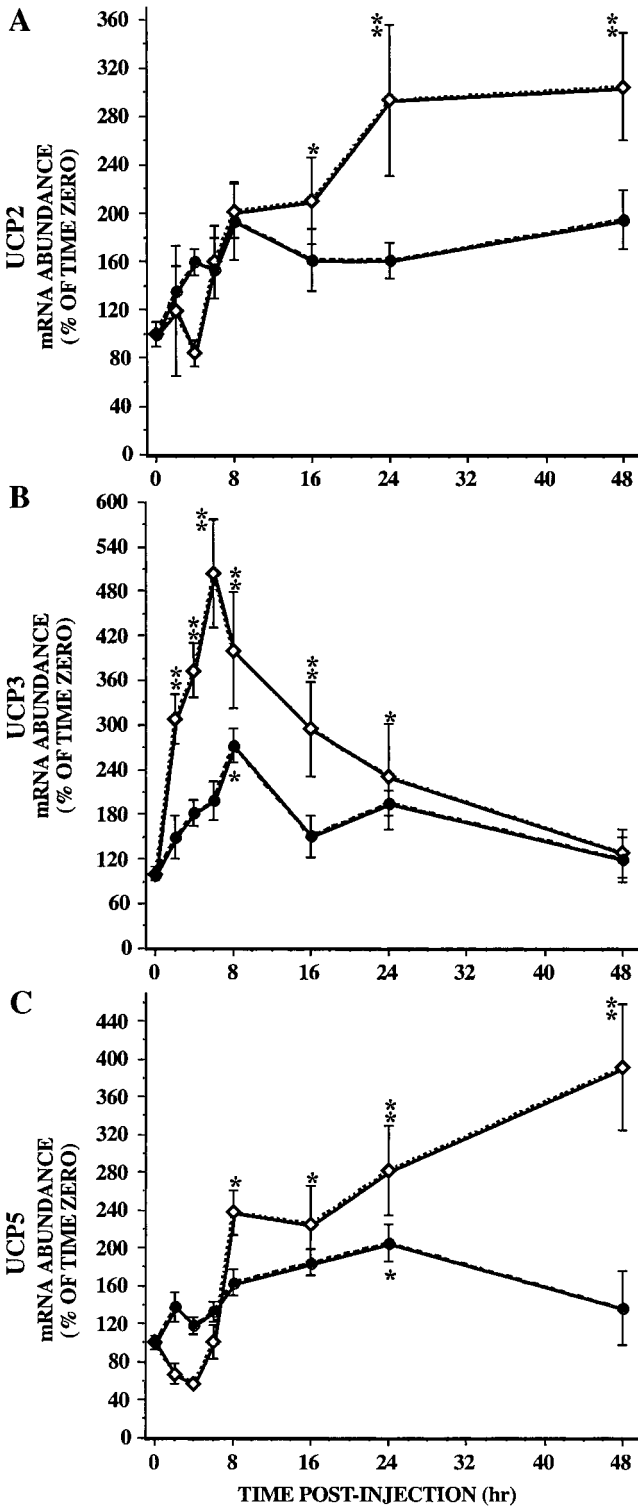


Fig. 2. Time-dependent stimulation of UCP homolog expression in hind-limb skeletal muscle (SKM) of LPS-treated mice. Determinations of UCP2 (A), UCP3 (B), and UCP5 mRNA abundance (C) were made on SKM derived from control (●) or LPS-treated (○) mice housed at 22°C (see Fig. 1 legend). Each point represents the mean ± SE of 3–5 independent measurements, derived from mice depicted in Fig. 1 (\**P* ≤ 0.05, \*\**P* ≤ 0.01 vs. *time 0* values); some error bars are within the symbol. Values for UCP2 mRNA at 8 h tended to be higher relative to *time 0* (*P* < 0.1). Not indicated are significant differences (*P* < 0.05) between LPS mice and time-matched controls, occurring at 2–6 and 16 h (UCP3) and at 48 h (UCP5) (no significant treatment × time interaction for UCP2).

hepatocyte-enriched pellet was snap-frozen. The pooled supernatants were centrifuged at 5,000 *g* for 10 min, and the NPC-enriched pellet was snap-frozen. This protocol using repeated washes yields a low-speed pellet containing >95% hepatocytes (1).

*Indirect calorimetry (study 5).* Twelve ad libitum-fed mice were acclimated for 24 h to respiration chambers (Oxymax System, Columbus Instruments, Columbus, OH). After acclimation, one-half of the mice were injected with LPS, and one-half served as PBS-injected controls (injection protocol as in *study 1*). The first postinjection measurement of  $\dot{V}O_2$  occurred ~1 h after injection and was followed hourly thereafter. *T<sub>c</sub>* was determined immediately after the 24-h postinjection chamber measurement. Mice were fasted after injection but were allowed free access to water.

*Statistics.* Changes in mRNA abundance and *T<sub>c</sub>* over time after injection were assessed by use of the general linear models procedure of SAS (SAS Institute, Cary, NC) as a 2 × 8 factorial design analyzing the effects of treatment (LPS vs. controls), time, and treatment × time interactions. Significant (*P* < 0.05) time or treatment × time interactions were observed for all parameters; however, individual comparisons between time-matched control vs. LPS-treated mice (see figure legends) were made only if treatment × time effects were significant. Means ± SE are reported.

RESULTS

*Study 1: LPS-evoked temperature, UCP homolog, and PGC-1 mRNA changes.* The administration of a ~6 mg/kg dose of endotoxin induced a profound hypothermia in mice (Fig. 1A). *T<sub>c</sub>* fell to 34°C by 4 h after injection, dropping further to a nadir of ~30°C by 8 h after injection. Although there was a decline in *T<sub>c</sub>* by

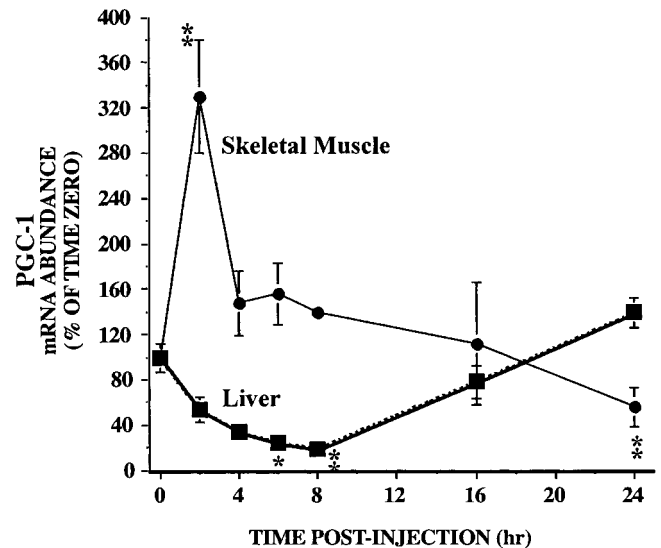
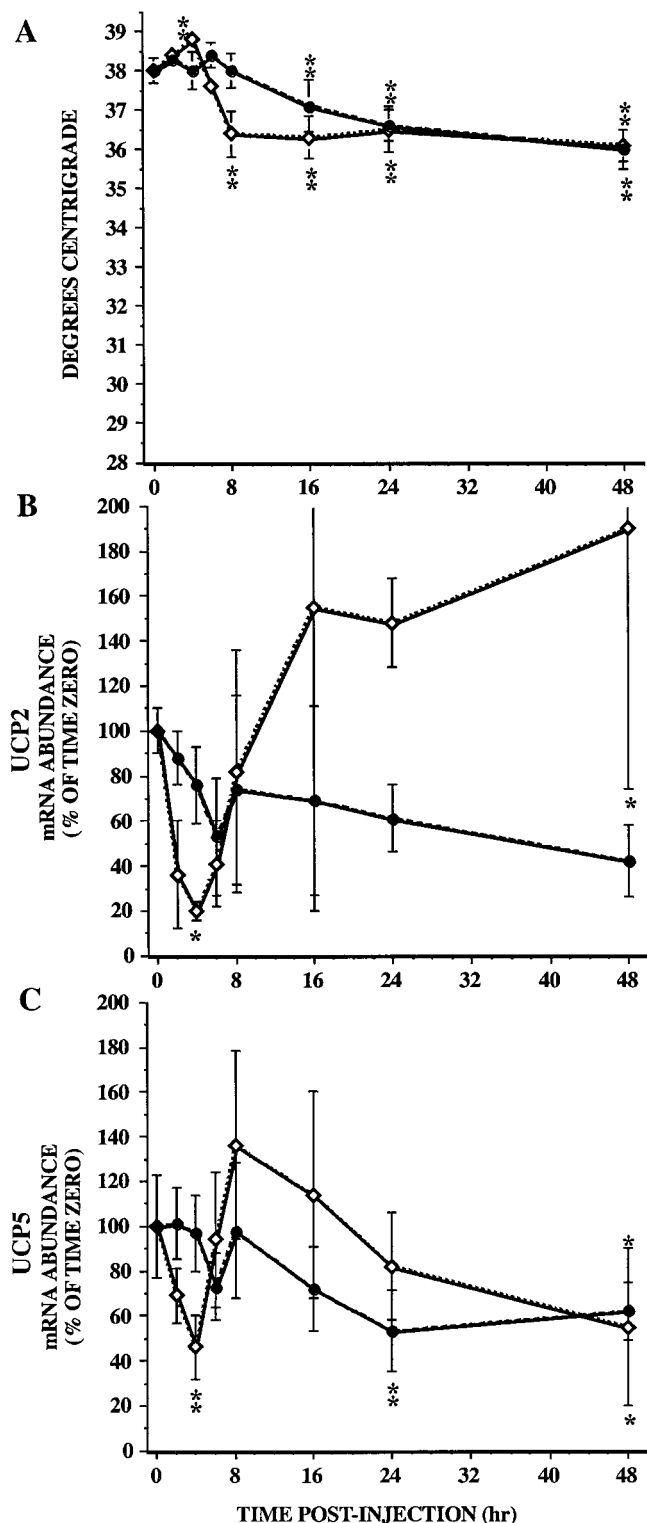


Fig. 3. Tissue-dependent stimulation or repression of peroxisome proliferator-activated receptor-γ coactivator 1 (PGC-1) expression in mice administered LPS. PGC-1 mRNA abundance was determined in a subset of SKM (●) and whole liver (■) samples from mice treated with LPS (samples are the same as those whose data are presented in Figs. 1 and 2). Three independent samples were used at each time point (\**P* ≤ 0.05, \*\**P* ≤ 0.01 vs. *time 0* values); some error bars are within the symbol. The drop in liver mRNA was apparent by 2 h (*P* = 0.06). Not shown are PBS-injected control values, which were not altered significantly relative to *time 0*.

2 h, this change was not statistically significant. Individuals sampled at 24 and 48 h after injection displayed a robust recovery of  $T_c$ , with a slight overshoot above time-matched controls by 48 h (Fig. 1A). Both control and LPS-treated mice were fasted after injection, and this led to a significant drop in  $T_c$  in controls by 16 h, remaining low through 48 h.



UCP homolog mRNA abundance in the liver was blunted sharply and rapidly after LPS administration (Fig. 1, B and C), with 2 h postinjection values only ~20–25% of controls. Transcript amount for each began to rise between 6 and 8 h after injection and were no different from time-matched controls at the 16-h time point. Hepatic UCP2 mRNA levels rose further between 16 and 24 h, remaining elevated compared with time-matched controls (Fig. 1B). In the latter, fasting elicited a significant drop in UCP2 and UCP5 mRNA by 16–24 h (Fig. 1, B and C). Based on real-time RT-PCR analysis of time-zero control samples, whole liver mRNA expression of UCP2 was about twofold higher than UCP5 (not shown). The magnitude of change in rodent liver UCP2 mRNA after LPS in the current study using quantitative RT-PCR is less than that reported by researchers who used Northern blot analysis (11, 12, 14), likely caused by differences in experimental regimens and our use of a more sensitive analytical methodology.

Skeletal muscle patterns of UCP2 and UCP5 mRNA abundance after LPS administration differed substantially compared with liver (Fig. 2, A-C). For instance, the decline in UCP5 mRNA over the first 4 h after injection was not statistically significant (Fig. 2C), and an LPS-induced decline in UCP2 expression was not apparent (Fig. 2A). In contrast to the liver pattern, SKM UCP5 mRNA in LPS-treated mice rose significantly above controls, reaching levels more than threefold higher than time-zero amounts by 48 h after injection (Fig. 2C). Furthermore, a fasting-induced drop in UCP2 or UCP5 transcript was not seen in SKM from control mice (Fig. 2, A and C). Interestingly, however, the mRNA levels for UCP2 and UCP5 began to rise between 6 and 8 h after LPS (Fig. 2, A and C), an induction reminiscent of that seen in liver (Fig. 1, B and C). As in liver, SKM UCP2 mRNA increased significantly above control values between 16 and 48 h in LPS-treated mice (Fig. 2A).

The UCP3 mRNA changes observed in SKM after LPS were markedly different relative to those observed for UCP2 and UCP5 (Fig. 2, A-C). After injection, there was an immediate and substantial induction of the UCP3 gene as judged by mRNA abundance, reaching levels more than fivefold above

Fig. 4. Whole liver patterns of UCP homolog mRNA abundance after prevention of hypothermia in LPS-treated mice. Adult female C57BL/6J mice were treated between 1530 and 1630 with a single ip dose of PBS (controls, ●) or LPS (◇) and housed at an ambient temperature of 34°C with fasting (*study 2*, see MATERIALS AND METHODS). Colonic temperature (A), liver UCP2 mRNA abundance (B), and liver UCP5 mRNA abundance (C) were determined in groups of mice through 48 h postinjection. Each point represents the mean  $\pm$  SE of 3–4 independent measurements (\* $P \leq 0.05$ , \*\* $P \leq 0.01$  vs. *time 0* values); some error bars are within the symbol. The lower values for UCP2 at 2 and 6 h after LPS ( $P < 0.1$ ) did not achieve statistical significance. Not indicated are significant differences ( $P < 0.05$ ) between LPS mice and time-matched controls, occurring at 4–16 h (body temperature), 16–48 h (UCP2), and 2 h (UCP5).

time-zero controls by 6 h (Fig. 2B). Levels tapered off over the remaining hours to equal those of time-matched controls by 24 h after injection, an event concurrent with time-dependent increases in UCP2 and UCP5 mRNA (see above). The rise in UCP3 mRNA in fasted controls was transient. In data not shown, RT-PCR detection values in SKM from time-

zero controls revealed that expression of UCP3 exceeded that of UCP2 and UCP5 by ~4- and >30-fold, respectively. UCP2 mRNA abundance was about fourfold higher in SKM than liver, whereas UCP5 was similar between tissues.

Exploration of the molecular basis of the remarkable UCP homolog expression changes noted over the first 24 h after injection of LPS (see above) prompted analysis of PGC-1 mRNA abundance in a subset of samples from these same mice. In liver, LPS significantly depressed PGC-1 up to fivefold in a time-dependent manner, with eventual recovery of transcript levels between 8 and 16 h after injection (Fig. 3). In contrast, PGC-1 mRNA abundance had risen more than threefold by 2 h after injection in SKM from LPS-treated mice, falling significantly to reach levels not statistically different from time-zero controls between 4 and 16 h (Fig. 3). In time-zero control tissues, mRNA abundance for PGC-1 in whole liver was ~2- and ~10-fold lower than that determined in SKM and BAT, respectively (not shown).

*Study 2: effect of core body temperature clamp on LPS-induced expression changes.* It was intriguing to note that induction of UCP homolog expression in liver and SKM in *study 1*, clear by 6–8 h after injection of LPS, occurred when core body temperature had approached or reached its nadir (see Figs. 1 and 2). Although these events may simply be coincidental, one may consider a paradigm in which signals emanating from core body temperature ( $T_{\text{core}}$ )-sensitive neurons in the brain act to modulate peripheral cellular heat production. Were the delayed UCP homolog gene expression increases observed after LPS “triggered” by low  $T_{\text{core}}$ , and would such increases be blunted should  $T_{\text{core}}$  be clamped to near-control temperature? As an initial test of this hypothesis, a second set of LPS and control mice was placed in a warm room (34°C) after injection, thus preventing the large drop in  $T_c$  displayed in *study 1* (compare Figs. 1A and 4A).

This treatment did not alter most patterns of UCP homolog mRNA changes (Figs. 4 and 5). For example, liver UCP2 and UCP5 mRNAs in LPS-treated mice dropped and then recovered to exceed or equal control values, respectively (Fig. 4, B and C), similar to what was observed at 22°C (Fig. 1, B and C). As in studies performed at 22°C (Fig. 2B), SKM UCP3

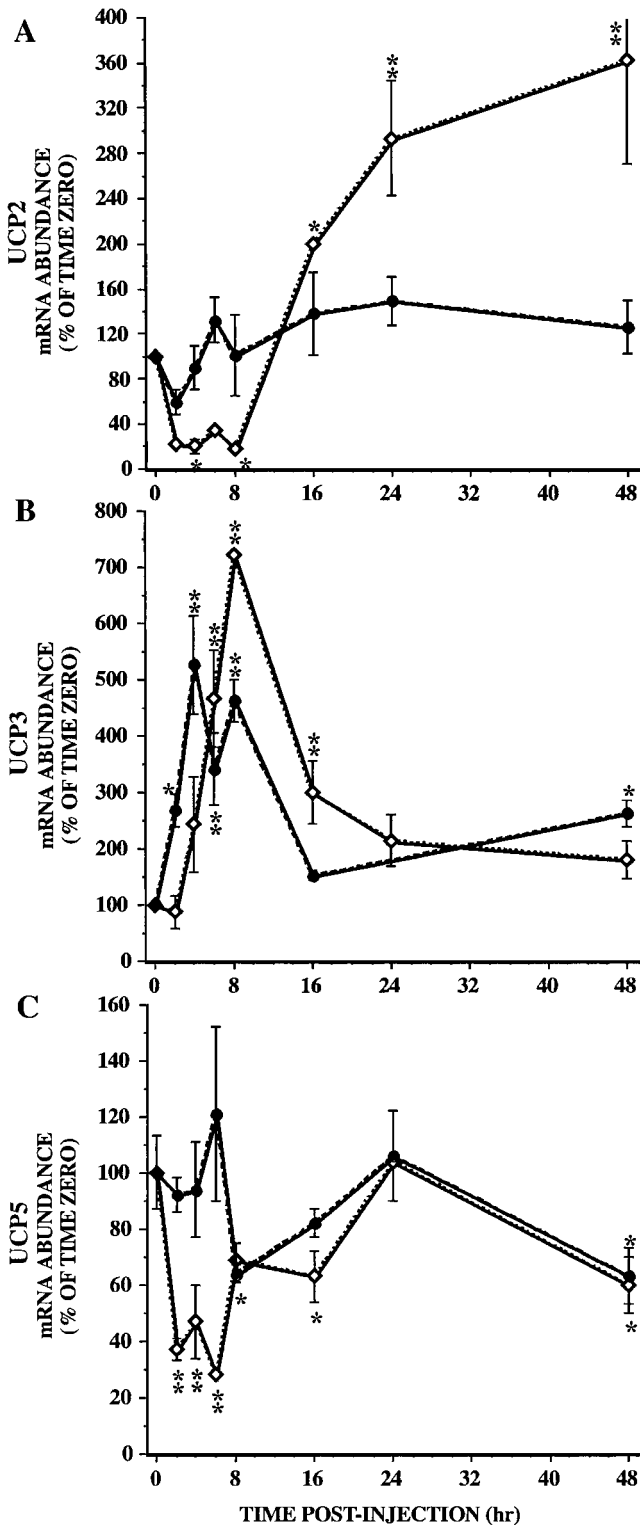


Fig. 5. Hindlimb SKM patterns of UCP homolog mRNA abundance after prevention of hypothermia in LPS-treated mice. Determinations of UCP2 (A), UCP3 (B), and UCP5 mRNA abundance (C) were made on SKM derived from control (●) or LPS-treated (◇) mice housed at 34°C (see Fig. 4 legend for details). Each point represents the mean ± SE of 3–4 independent measurements (\* $P \leq 0.05$ , \*\* $P \leq 0.01$  vs. *time 0* values); some error bars are within the symbol. Values for UCP2 at 2 and 6 h ( $P < 0.1$ ), UCP5 at 8 h ( $P = 0.06$ ), and increased UCP3 at 4 h ( $P = 0.06$ ) post-LPS clearly differed from *time 0* values but did not achieve statistical significance at  $P < 0.05$ . Not indicated are significant differences ( $P < 0.05$ ) between LPS mice and time-matched controls, occurring at 6–8 and 24–48 h (UCP2), 2–4 and 8 h (UCP3), and 2–6 h (UCP5).

transcript in temperature-clamped LPS-treated mice increased significantly (albeit with more of a delay) and then fell in a time-dependent manner (Fig. 5B). Generally, control patterns of UCP homolog expression were similar in both studies, although the increase in UCP3 mRNA in fasted control SKM appeared to be higher and of longer duration at 34°C (compare Figs. 2B and 5B). Despite such similarities, there were notable differences in expression between the studies. Although a significant and delayed induction of UCP2 mRNA in SKM in LPS-treated mice was seen in both 22°C and 34°C studies (compare Figs. 2A and 5A), a substantial transient fall in UCP2 expression was observed only at 34°C (Fig. 5A). The pattern for UCP5 mRNA in the mice given LPS was generally similar (compare Figs. 2C and 5C); however, the magnitude of the delayed induction in UCP5 mRNA abundance was blunted at 34°C (Fig. 5C).

*Study 3: mitochondrial proton leak after LPS treatment.* Marked alterations in body temperature and UCP homolog gene expression after LPS treatment (Figs. 1 and 2) suggested that significant time-dependent changes in mitochondrial uncoupling kinetics, an expected functional correlate of UCP activity, could have occurred in endotoxin-challenged mice. To assess this possibility, mitochondrial proton leak in LPS-injected mouse liver was assayed in parallel with control liver mitochondria at time points corresponding to diminution and recovery of UCP2 and UCP5 expression (4 and 16 h, respectively; Fig. 1, B and C). Liver samples used for proton leak measurements yielded an expression pattern matching that of the initial study (significant drop in UCP2 and UCP5 mRNA at 4 h post-LPS, recovery to control levels by 16 h; not shown). An LPS-induced  $T_c$  decline was again observed at 4 h (controls,  $37.0 \pm 0.18^\circ\text{C}$ ; LPS,  $34.9 \pm 0.34^\circ\text{C}$ ;  $n = 9/\text{treatment}$ ) and 16 h (controls,  $34.5 \pm 0.32^\circ\text{C}$ ; LPS,  $25.8 \pm 0.41^\circ\text{C}$ ;  $n = 24/\text{treatment}$ ) resembling that of the initial study (Fig. 1A). Despite large changes in mRNA abundance and  $T_c$  in this group of mice (similar to mice in *study 1*), no significant difference in liver mitochondrial respiration due to proton leak between treatments was discernible under our assay conditions (Fig. 6, A and B). Similarly, no suggestion of proton leak differences was evident in SKM mitochondria at 16 h after injection (not shown).

To gather additional insight into the physiological relevance of proton leak in hypothermic mice, a subset of LPS mitochondria used for the 16-h analyses described above was also assayed at 26°C. This temperature corresponds to the average  $T_c$  of LPS-treated mice (see above) and is therefore more likely to reflect the kinetics of proton leak in mitochondria from these animals in situ compared with assays performed at 37°C. At this cooler temperature, oxygen consumption due to proton leak was a fraction of that observed in control or LPS mitochondria assayed at 37°C, despite increased estimated membrane potentials overall (Fig. 6C).

*Study 4: hepatocyte expression of UCP homologs.* It has been reported that, in rodent liver, UCP2 expression in hepatocytes is minor compared with that in the far less abundant Kupffer cells (11, 12, 26). This issue is relevant to interpretation of correlations between proton leak and whole liver UCP homolog mRNA abundance, because the contribution of NPC mitochondria to preparations used for proton leak is vanishingly small compared with the contribution from hepatocytes (2). In addition, the cell-specific expression of UCP5 or PGC-1 in liver has not been reported. To address these issues, mRNA was analyzed from hepatocyte-enriched preparations<sup>1</sup> derived from a separate set of control or LPS-treated mice at time points corresponding to proton leak measurements made in mice used for *study 3*. As seen for whole liver (Fig. 1, B and C), hepatocyte UCP2 and UCP5 mRNA dropped substantially by 4 h after injection of LPS, with UCP5 mRNA recovering to control values by 16 h (Fig. 7, A and B). However, hepatocyte UCP2 expression was not increased by 16 h in this group of mice. Hepatocytes expressed PGC-1 (Fig. 7C), with the drop in mRNA after LPS administration similar to the pattern observed in whole liver (Fig. 3).

*Study 5: oxygen consumption after LPS administration.* The profound hypothermic response and subsequent body temperature recovery in LPS-treated mice (Fig. 1A) indicated that substantial changes in metabolic heat production occur in these animals over the first 24 h after LPS. As a functional corollary to in vitro observations of UCP homolog expression and mitochondrial proton leak, metabolic rate was assessed by indirect calorimetry in mice injected with saline or LPS. Compared with mice from *study 1* (e.g., Fig. 1A), animals from this group displayed substantial variation in their metabolic response to endotoxin (Fig. 8). In all but one animal (*age 2*, see Fig. 8 legend),  $\dot{V}_{O_2}$  began to diverge from control mice between 3 and 4 h after injection with a progressive and marked hypometabolism occurring from 4 h onward. One animal (*age 12*) exhibited a partial recovery of  $\dot{V}_{O_2}$  beginning by ~16 h (Fig. 8). Importantly, differences in  $\dot{V}_{O_2}$  were

<sup>1</sup> Compared with the NPC fraction (see MATERIALS AND METHODS), the hepatocyte-enriched fraction contained >50-fold less transcript for the macrophage-specific marker F4/80 (30), indicating that Kupffer contamination was negligible. The focus of this study was to assess expression changes in purified hepatocytes and was not designed as a formal examination of UCPs in NPCs. Therefore, cells in the NPC-enriched fraction were not separated further. Nonetheless, it is notable that the NPC-enriched fractions consistently contained at least two- to fourfold higher UCP2 mRNA abundance than the hepatocyte-enriched fraction (not shown). These findings are consistent with far greater expression of UCP2 in NPCs relative to hepatocytes (11, 12, 26), because the contribution of NPC mRNA in the NPC-enriched fraction was largely diluted by significant contaminating hepatocyte mRNA (albumin transcript was about equal between fractions; not shown). UCP5 mRNA was detected about equally in both fractions; thus the UCP5 mRNA in the NPC-enriched fraction was largely due to the contribution of hepatocyte mRNA (see above). However, such preliminary findings cannot rule out the possibility that UCP5 is also expressed in NPCs.

reflected by  $T_c$  measures taken at 24 h after injection: controls ( $33.9 \pm 0.6^\circ\text{C}$ ,  $n = 6$ ), hypometabolic mice ( $24.6 \pm 0.22^\circ\text{C}$ ,  $n = 4$ ), the *cage 2* mouse ( $34.2^\circ\text{C}$ ), and the *cage 12* mouse ( $28.6^\circ\text{C}$ ).

DISCUSSION

*Association of UCP homolog expression and metabolic outcomes.* Whether newly described or still undiscovered mitochondrial carrier proteins act to uncouple mitochondrial respiration analogous to UCP1 is actively being investigated. There is an abundance of information regarding UCP homolog expression changes under various metabolic conditions, but few studies have correlated such changes with functional metabolic outcomes in rodents (11, 21, 24, 38, 39). The current set of experiments was centered on the premise that, should a particular UCP homolog act as an uncoupler *in situ*, robust modulation of its expression *in vivo* should elicit concurrent detectable changes in functional outcomes, including metabolic heat production and mitochondrial proton leak. Analyses described herein focused on liver and SKM, which are believed to account for over one-half of the metabolic rate of rodents (9).

Based on mRNA patterns alone, certain aspects of UCP2 and UCP5 expression in the current model are consistent with the view that these homologs contribute to uncoupling *in vivo*. First, development of hypothermia in LPS-treated mice was preceded by a drop in liver UCP2 and UCP5 mRNA abundance (Fig. 1), and under normal conditions the liver's contribution to metabolic rate is significant (9). The failure of LPS to diminish UCP2 or UCP5 expression in SKM during hypothermia (Fig. 2), however, suggests that any putative impact of these homologs on diminution of heat production would not have been manifested in SKM. Second, recovery of  $T_c$  was preceded by significant increases in UCP2 and UCP5 expression in liver and SKM (Figs. 1 and 2), consistent with the hypothesis that increased activity of these homologs contributed to reestablishment of  $T_c$  after LPS. The significant lag between UCP2 and UCP5 expression changes (beginning at ~6–8 h after injection, Figs. 1 and 2) and the recovery of  $T_c$  to control levels (between 16 and 24 h after injection, Fig. 1) do not preclude the possibility that these proteins are involved in  $T_c$  recovery after LPS, because a sustained rise in energy expenditure would have been required to normalize the  $T_c$  of hypothermic mice. For example, an increase of  $4^\circ\text{C}$  in a 17-g mouse over a period of 8 h (Fig. 1) would have required

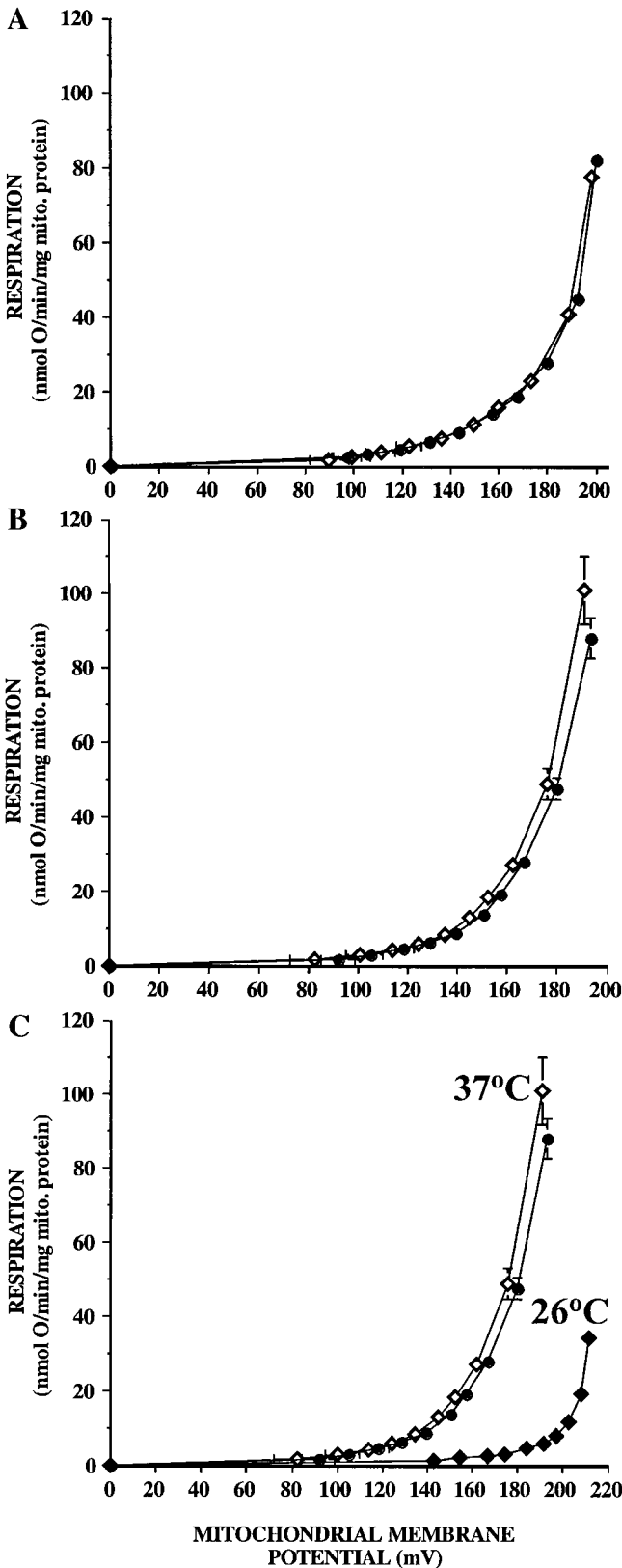


Fig. 6. Lack of effect of *in vivo* LPS treatment on liver mitochondrial proton leak kinetics in mice. Respiration attributable to liver mitochondrial proton leak was measured at various titrations of mitochondrial membrane potential in isolated organelles derived from adult female C57BL6/J mice injected ip with PBS (controls, ●) or LPS (◇) between 1530 and 1630 (*study 3*, see MATERIALS AND METHODS). Graphs correspond to measurements taken beginning at 4 h (A) or at 16 h (B and C) postinjection. Data in (C) illustrate the alteration of proton leak that occurred in a subset ( $n = 3$ ) of 16-h LPS-treated mouse preparations assayed at  $26^\circ\text{C}$  (◆) vs. kinetics of mitochondria assayed at the typical  $37^\circ\text{C}$  [data from (B) are reproduced in (C) for comparison]. Symbols represent mean values for independent experiments at any given titration point in the assay ( $n = 3/\text{treatment at 4 h}$ ,  $n = 7/\text{treatment at 16 h}$ ), with SEs for respiration and membrane potentials indicated by vertical and horizontal error bars, respectively; some error bars are within the symbol.

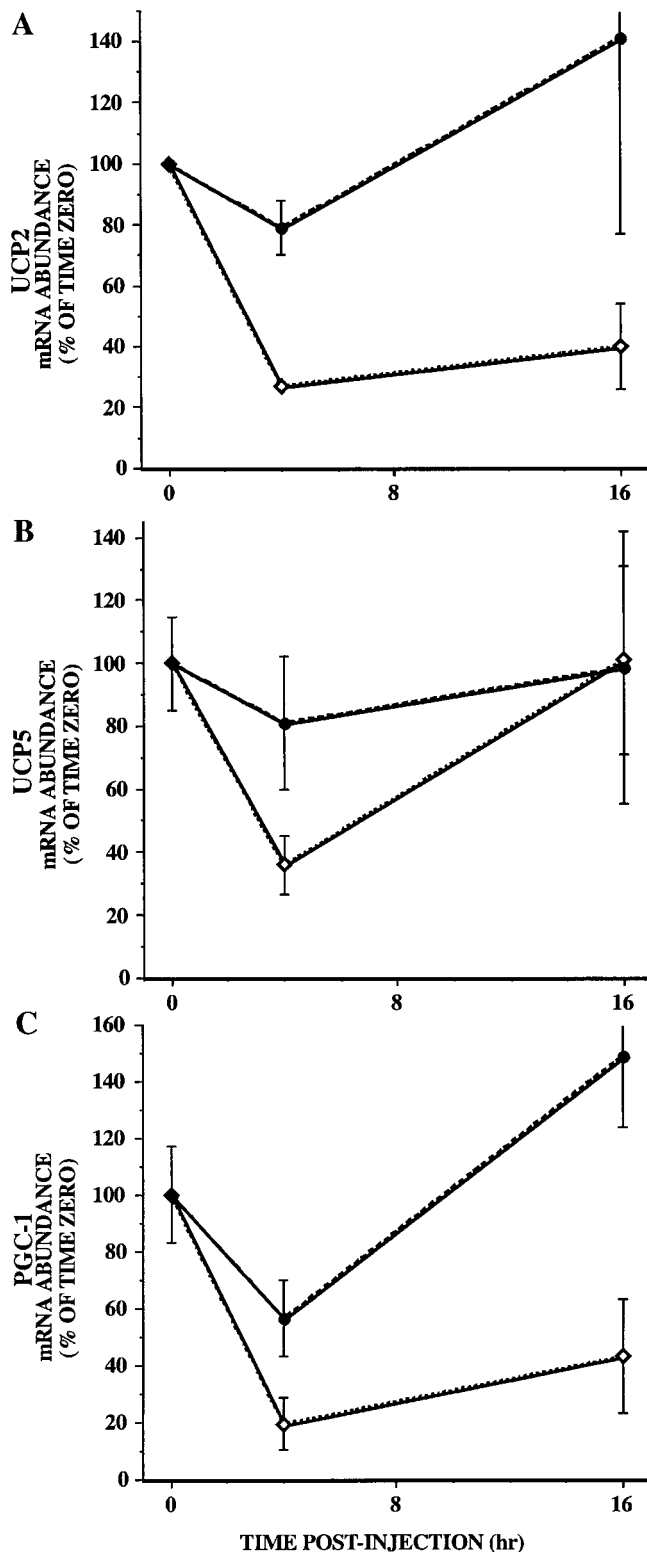


Fig. 7. Depression of UCP homolog and PGC-1 mRNA in hepatocytes isolated from LPS-treated mice. At each time point depicted, hepatocyte-enriched cell fractions were obtained from adult female C57BL6/J mice injected with PBS (controls, ●) or LPS (◇) (study 4, see MATERIALS AND METHODS). Values at each time point represent the mean mRNA abundance of UCP2 (A), UCP5 (B), or PGC-1 (C) from 2 independent preparations/treatment.

the generation and full sequestration of  $\sim 60$  calories just to account for the temperature rise.<sup>2</sup> This is an underestimate of the actual energy needs to accomplish this feat, because it does not take into account the loss of metabolic heat via respiration and other routes. Furthermore, mitochondrial proton leak kinetics slow considerably at cooler temperatures (Fig. 6C). Thus truly effective activities of putative UCP homologs are not likely to parallel expression changes in hypothermic animals, and would manifest themselves fully only as mice begin to warm.

Expression patterns of UCP3 in SKM (Fig. 2B) raise questions about the relevance of UCP3 toward driving truly meaningful heat production changes in LPS-treated mice, and they lend support to the idea that this homolog has other primary functions in vivo (e.g., Refs. 38, 39, 44). For instance, UCP3 transcript levels in SKM were rapidly triggered fivefold by LPS administration (Fig. 2), rising concurrently with the drop in body temperature (the latter tracked metabolic rate, see RESULTS). On the other hand,  $T_c$  recovery was accompanied by diminishing UCP3 mRNA levels.

Regardless of the roles of UCP homologs in modifying in situ uncoupling, tissue proton leak could not have been the only factor contributing to hypometabolism after LPS. The four- to eightfold drop in  $\dot{V}O_2$  (Fig. 8) and the magnitude of decline in  $T_c$  (Fig. 1) caused by LPS appear too large to be accounted for by changes in proton leak alone, which under basal conditions may represent up to  $\sim 20$ – $40\%$  of tissue  $\dot{V}O_2$  in rodents (9). Global depression of metabolism, including a diminution of reactions generating and consuming the mitochondrial electrochemical gradient, likely occurs after high-dose LPS administration to mice. For example, although not measured in the current study, endotoxin has been shown to increase nitric oxide (NO) production (27, 41), and NO or its derivatives powerfully inhibit the electron transport chain (36). Furthermore, mice developing hypothermia after LPS (Fig. 1) displayed a marked reduction in motor activity (23). Thus, regardless of any possible changes in proton leak, LPS-induced diminution of ATP consumption or depression of the  $\Delta\psi$  generating pathways would contribute to alterations of metabolic rate and body temperature.

Despite large alterations of  $T_c$  (Fig. 1), metabolic rate (Fig. 8), and UCP homolog mRNA in liver (Figs. 1 and 7) and SKM (Fig. 2), no discernible difference in proton leak could be detected in mitochondria prepared from liver (Fig. 6) or SKM (see RESULTS). Recently, a lack of correlation was reported between leak and liver/SKM UCP2 and SKM UCP3 mRNA in mice administered thyroid hormone or after a fast (9a, 21). A lack of correlation between in vitro proton leak assays and UCP homolog mRNA abundance could signal that the primary physiological role of UCP2, UCP3, and UCP5 is not to catalyze mitochondrial proton leak per se but

<sup>2</sup> Calculation of energy requirements to raise body temperature assumed a heat capacity of  $3.66 \text{ kJ} \cdot \text{kg}^{-1} \cdot ^\circ\text{C}^{-1}$  for normal mice (13) and a conversion factor of  $4.184 \text{ J/cal}$ .

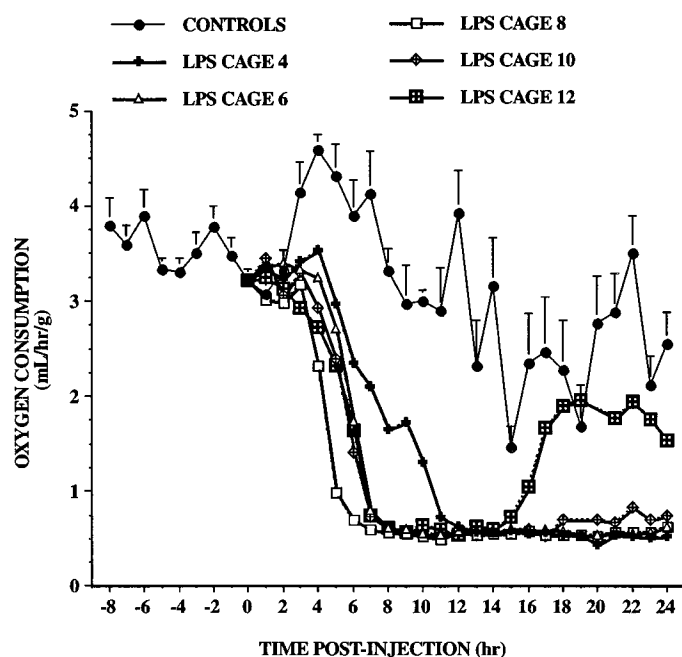


Fig. 8. Metabolic depression in mice injected with endotoxin. Metabolic rate was determined via indirect calorimetry in adult female C57BL6/J mice before and after ip injection of PBS (controls, ●) or LPS (other symbols) between 1430 and 1530 (0 h), after which animals were fasted (*study 5*, see MATERIALS AND METHODS). Control values represent the mean  $\pm$  SE of all mice at  $-8$  to  $0$  h ( $n = 12$ ) or those injected with PBS at 1-h postinjection onward ( $n = 6$ ). Data on individual LPS-treated mice are shown separately to highlight individual variation observed after treatment in this particular group of animals. Not shown is a single LPS-treated mouse (*case 2*) that for unclear reasons did not display a drop in metabolic rate after injection (see RESULTS).

rather to serve as carriers for fatty acids or other moieties. Alternatively, it is possible that the commonly used assay conditions for measurement of mitochondrial proton leak employed in the current study do not adequately reflect leak kinetics *in vivo* under every condition and may therefore lead to negative interpretations of UCP homolog activity. In a recent study, Lanni et al. (24) noted that proton leak differences in SKM mitochondria derived from rats differing in thyroid status were observed only when assays were carried out free of BSA, suggesting involvement of fatty acids with proton leak. As noted by Porter et al. (32a), higher proton leak was observed in hepatocytes from aged rats compared with young rats, but such a difference was not apparent with the use of isolated mitochondria. Thus various factors, including fatty acids or purine nucleotides (e.g., Refs. 4, 19, 40), and perhaps protein modulators, may regulate UCPs in the context of the cell *in situ*. In addition, it is possible that changes in protein levels in the tissues examined herein were too small to enable detection of differences in proton leak despite alterations of mRNA. Finally, the possibility cannot be discounted that still uncharacterized mitochondrial carriers exist and importantly influenced proton leak in these tissues.

The variable results to date regarding UCP homolog expression and functional outcomes highlight the ne-

cessity for research to clarify further the metabolic roles of these proteins. Although we observed no differences in mitochondrial proton leak, despite remarkable alterations of UCP homolog gene expression in LPS-treated mice, increased proton leak was observed in mitochondria prepared from *ob/ob* mouse liver and hyperthyroid rat SKM that displayed increased hepatocyte UCP2 and SKM UCP3 expression, respectively (11, 24). Samec et al. (39) did not observe a correlation between UCP homolog mRNA abundance and whole animal  $\dot{V}O_2$  in a high-fat/low-fat model, whereas Jekabsons et al. (21) presented evidence of a positive association between muscle UCP2 and UCP3 expression changes and whole animal  $\dot{V}O_2$ . Our correlative data on  $T_c$  recovery and UCP2/UCP5 mRNA (Figs. 1 and 2) concur with this latter finding, because  $T_c$  tracks changes in  $\dot{V}O_2$  (see RESULTS), but they differ in that UCP3 mRNA changes generally followed a pattern opposite that of  $T_c$  (Fig. 2). Finally, others have reported increased rodent SKM UCP2 and UCP3 mRNA with fasting or food restriction (5, 6, 9a, 17, 20, 38, 44), but our results in fasting control mice indicated that UCP2 and UCP3 mRNA changes were transient and varied between *studies 1* and *2* (Figs. 2 and 5). Differences between our study and those of others could be related to our use of analytical mRNA methodology or to the fact that we initiated the injection and fasting regimen in late afternoon, a time point preceded by low food intake relative to the dark cycle.

**Gene regulation of UCP homologs.** LPS administration initiates a complex cascade of events in which an array of cytokines, prostaglandins, and other factors change temporally to influence metabolism (28). With respect to humoral, paracrine, or autocrine components that influenced UCP homolog expression in the first hours after LPS (Figs. 1 and 2), factors such as tumor necrosis factor- $\alpha$  (TNF- $\alpha$ ) and interleukin-1 $\beta$  that emerge early in the cascade are good candidates. Faggioni et al. (14) reported that a single injection of TNF- $\alpha$  to mice caused a two- to threefold increase in liver, SKM, and WAT UCP2 mRNA levels at 12 h, but changes at earlier time points were not reported. Indeed, a delay in liver UCP2 induction after LPS or TNF- $\alpha$  treatment has been consistently observed (11, 12, 14, this study). Thus a direct stimulation of UCP2 or UCP5 genes in mouse liver or SKM by TNF- $\alpha$  does not appear possible, because the transient nature of this cytokine dictates that its direct effects must occur in the first  $\sim 2$  h after LPS (47), when UCP2 and UCP5 mRNA levels were stable or falling (Figs. 1 and 2). Cytokines induced later in the LPS-induced cascade (28) or other humoral factors, such as the newly described high mobility group 1 (43), might have influenced the delayed induction of UCP2 and UCP5 in liver and SKM after LPS (Figs. 1 and 2).

The current study illustrates that, under certain conditions, the mechanisms controlling UCP2 and UCP5 genes may converge and that genetic regulation of UCP3 is markedly different from that of UCP2 or UCP5 after high-dose endotoxin in mice. For instance, LPS evoked a similar repression and recovery of UCP2

and UCP5 expression in liver (Figs. 1 and 4) plus a delayed induction in SKM (Figs. 2 and 5), contrasting with the early and transient induction of SKM UCP3 (Figs. 2 and 5). There is evidence that the availability of fatty acid-associated moieties (20, 44) stimulates expression of UCPs. Indeed, the availability of fatty acids likely influenced the expression of SKM UCP3 in the current study, as evidenced by a separate experiment in which plasma FFA levels plus UCP3 mRNA were determined at 0, 2, and 6 h after injection of LPS or PBS. A strong correlation between plasma FFA concentration and UCP3 expression was observed in LPS-treated mice (Fig. 9). Compared with time-matched controls, the 6-h postinjection FFA concentration ( $1.20 \pm 0.12$  mM) and SKM UCP3 expression ( $600 \pm 32\%$  of *time 0*) in LPS-treated mice was approximately two- and threefold greater. The mechanisms underlying the LPS-induced rise in circulating FFA levels and their association with UCP3 gene expression remain unknown.

Activation of PPAR $\gamma$  and/or PPAR $\alpha$  (10, 20, 22), and tissue-specific upregulation of the coactivator PGC-1 (34, 45), could influence UCP homolog expression. Studies examining the role of ectopic PGC-1 in C<sub>2</sub>C<sub>12</sub> cells and other *in vitro* preparations suggested that this coactivator is critical for the activation of the UCP1 and UCP2 genes, with little to no impact on UCP3 gene expression (34, 45). Interestingly, LPS sparked a significant increase in SKM PGC-1 expression (Fig. 3), which correlated well with initiation of UCP3 expression but was not associated with a change in UCP2 or UCP5 mRNA (Fig. 2). Thus it is intriguing

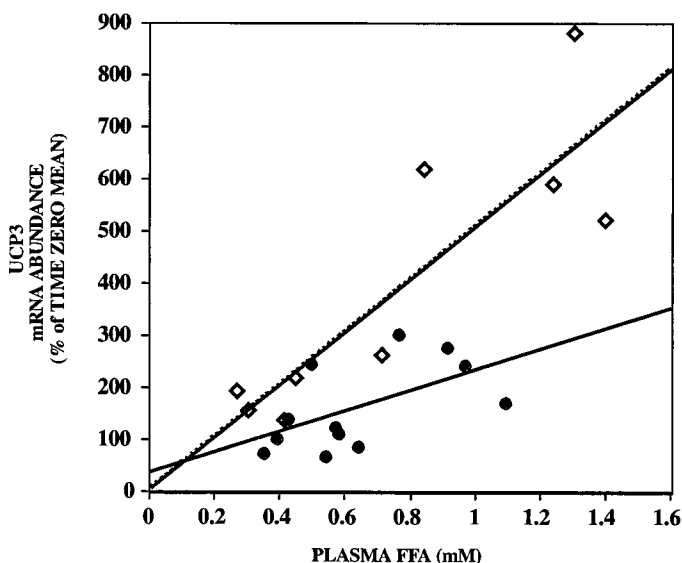


Fig. 9. UCP3 expression in SKM of LPS-treated mice correlates with a rise in plasma free fatty acid (FFA) concentration. Determinations of circulating FFA and hindlimb SKM UCP3 mRNA abundance were made in samples derived from adult female C57BL6/J mice injected ip with PBS (controls, ●) or LPS (◇). UCP3 mRNA was strongly correlated with plasma FFA in LPS mice ( $r^2 = 0.75$ ,  $P < 0.001$ /slope different from zero), whereas this relationship was not as apparent in controls ( $r^2 = 0.33$ ,  $P = 0.05$ /slope different from zero). Data points represent matched samples across all time points measured (0, 2, and 6 h postinjection; see DISCUSSION).

to postulate that SKM PGC-1 activity may influence the UCP3 gene in the context of the whole animal and may have influenced changes in UCP3 gene expression in LPS-treated mice. There was some disconnect between PGC-1 and UCP2 or UCP5 expression in whole liver, such that UCP homolog mRNA levels rose well before recovery of PGC-1 expression (Figs. 1 and 3). Recently, Boss et al. (3) reported that administration of  $\beta$ -adrenergic agonists or exposure to cold in wild-type or  $\beta_3$ -receptor knock-out mice could lead to increases in SKM UCP2 and UCP3 expression without concomitant changes in PGC-1 mRNA. Such examples of minimal correlation are not consistent with the idea that PGC-1 changes alone drive UCP2 or UCP5 expression *in vivo*, with the caveat that PGC-1 protein abundance was not measured (Ref. 3, this study). Using quantitative PCR, we found PGC-1 to be expressed in whole liver, hepatocytes, and SKM (Figs. 3 and 7), at odds with the data of Puigserver et al. (34), which indicated nominal expression in liver or SKM (PGC-1 could be induced by cold in the latter tissue) using Northern analysis. These discrepancies are likely explained by technical differences in sensitivity, because PGC-1 expression using real time RT-PCR was far greater (10-fold) in mouse BAT than liver (see RESULTS), consistent with Puigserver et al. Results to date (3, 34, 45, this study) indicate that the relative impact of PGC-1 activity on genes encoding UCP family members largely depends on the specific cell type, UCP homolog, and biological context of the system in study (i.e., whether or not PPAR $\gamma$  is activated by ligand). It is clear that additional regulatory mechanisms exist that modify UCP genes independently of changes in PGC-1 expression alone.

Exposure to cold ambient temperature ( $T_a$ ) is a powerful stimulus that engages the metabolic machinery of mammals, including  $\beta$ -adrenergic stimulation of BAT thermogenic activity (4). There is some evidence that a cold  $T_a$  induces UCP homolog expression in a tissue-dependent manner (reviewed in Ref. 4; see also Ref. 46). We are unaware of any reports that have studied the effects of core body temperature ( $T_{core}$ ) on UCP homologs, and we wondered whether experimental modulation of  $T_{core}$  would elicit changes in their expression levels. One hypothesis, for instance, is that the drop in  $T_{core}$  after LPS administration in mice (Fig. 1) may have stimulated the genes encoding UCP2 and UCP5 (Figs. 1 and 2) via  $T_{core}$  sensors that communicate with the brain. Teleologically, a hypothermia-induced enhancement of thermogenic uncoupling activity via UCP homologs could help counteract an excessive  $T_{core}$  drop. Artificial maintenance of  $T_{core}$  after LPS would be expected to dampen any cold-stimulated rise in UCP homolog expression. In an initial test of this hypothesis, clamping of  $T_{core}$  after LPS challenge generally failed to blunt the delayed stimulation of UCP2 and UCP5 gene expression, with the possible exception of SKM UCP5, whose induction was lower compared with that seen at 22°C (Figs. 3 and 4). These findings indicate that regulatory factors independent of  $T_{core}$  were at play in our LPS model.

In summary, some aspects of the current set of experiments are supportive of the idea that UCP2 and UCP5 are involved in metabolic changes occurring in LPS-treated mice. mRNA for these homologs was induced in whole liver and SKM during recovery from LPS-induced hypothermia, and in liver, their transcript levels dropped during the onset of hypothermia. Despite these patterns, no difference was observed in *in vitro* mitochondrial proton leak. Alterations in SKM UCP3 mRNA after endotoxin were distinctly different from those observed for UCP2 or UCP5, changing in the opposite direction from body temperature. These data point to different mechanisms of gene regulation and suggest that UCP3 does not serve in a thermogenic capacity under these conditions. Changes in expression of the transcription coactivator PGC-1 in muscle appeared to correlate with UCP3 expression, whereas the association between PGC-1 and UCP2 was less compelling. Further study is warranted to assess the possibility that LPS-induced increases in UCP homolog expression/activity help minimize LPS-associated reactive oxygen species production and damage. Ultimately, titration of UCP homolog abundance through gene delivery, transgenic construction, and knock-out technologies promises to clarify further the physiological roles of these proteins.

The authors thank E. Filvaroff and T. A. Stewart for helpful discussions of the manuscript, M. Renz for significant technical input, and C. Galindo and M. Ostland for statistical assistance.

## REFERENCES

- Berry MN, Edwards AM, and Barritt GJ. *Isolated Hepatocytes. Preparation, Properties, and Applications*. New York: Elsevier, 1991.
- Blouin A, Bolender RP, and Weibel ER. Distribution of organelles and membranes between hepatocytes and nonhepatocytes in the rat liver parenchyma. *J Cell Biol* 2: 441–445, 1977.
- Boss O, Bachman E, Vidal-Puig A, Zhang CY, Peroni O, and Lowell BB. Role of  $\beta_3$ -adrenergic receptor and/or a putative  $\beta_4$ -adrenergic receptor on the expression of uncoupling proteins and peroxisome proliferator-activated receptor- $\gamma$  coactivator-1. *Biochem Biophys Res Commun* 261: 870–876, 1999.
- Boss O, Muzzin P, and Giacobino J-P. The uncoupling proteins, a review. *Eur J Endocrinol* 139: 1–9, 1998.
- Boss O, Samec S, Dulloo A, Seydoux J, Muzzin P, and Giacobino J-P. Tissue-dependent upregulation of rat uncoupling protein-2 expression in response to fasting or cold. *FEBS Lett* 412: 111–114, 1997.
- Boss O, Samec S, Kuhne F, Bijlenga P, Assimakopoulos-Jeannet F, Seydoux J, Giacobino J-P, and Muzzin P. Uncoupling protein-3 expression in rodent skeletal muscle is modulated by food intake but not by changes in environmental temperature. *J Biol Chem* 273: 5–8, 1998.
- Boss O, Samec S, Paoloni-Giacobino A, Rossier C, Dulloo A, Seydoux J, Muzzin P, and Giacobino J-P. Uncoupling protein 3: a new member of the mitochondrial carrier family with tissue-specific expression. *FEBS Lett* 408: 39–42, 1997.
- Bouillaud F, Weissenbach J, and Ricquier D. Complete cDNA-derived amino acid sequence of rat brown fat uncoupling protein. *J Biol Chem* 261: 1487–1490, 1986.
- Brand MD, Chien L-F, Ainscow EK, Rolfe DFS, and Porter RK. The causes and functions of mitochondrial proton leak. *Biochim Biophys Acta* 1187: 132–139, 1994.
- Cadenas S, Buckingham JA, Samec S, Seydoux J, Din N, Dulloo AG, and Brand MD. UCP2 and UCP3 rise in starved rat skeletal muscle but mitochondrial proton conductance is unchanged. *FEBS Lett* 462: 257–260, 1999.
- Camirand A, Marie V, Rabelo R, and Silva JE. Thiazolidinediones stimulate uncoupling protein-2 expression in cell lines representing white and brown adipose tissues and skeletal muscle. *Endocrinology* 139: 428–431, 1998.
- Chavin KD, Yang S, Lin HZ, Chatham J, Chacko VP, Hoek JB, Walajts-Rode E, Rashid A, Chen C-H, Huang C-C, Wu T-C, Lane MD, and Diehl AM. Obesity induces expression of uncoupling protein-2 in hepatocytes and promotes liver ATP depletion. *J Biol Chem* 274: 5692–5700, 1999.
- Cortez-Pinto H, Yang SQ, Lin HZ, Costa S, Hwang C-S, Lane MD, Bagby G, and Diehl AM. Bacterial lipopolysaccharide induces uncoupling protein-2 expression in hepatocytes by a tumor necrosis factor- $\alpha$ -dependent mechanism. *Biochem Biophys Res Commun* 251: 313–319, 1998.
- Faber P and Garby L. Fat content affects heat capacity: a study in mice. *Acta Physiol Scand* 153: 185–187, 1995.
- Faggioni R, Shigenaga J, Moser A, Feingold KR, and Grunfeld C. Induction of UCP2 gene expression by LPS: a potential mechanism of increased thermogenesis during infection. *Biochem Biophys Res Commun* 244: 75–78, 1998.
- Fleury C, Neverova M, Collins S, Raimbault S, Champigny O, Levi-Meyrueis C, Bouillaud F, Seldin MF, Surwit RS, Ricquier D, and Warden CH. Uncoupling protein-2: a novel gene linked to obesity and hyperinsulinemia. *Nat Genet* 15: 269–272, 1997.
- Gimeno RE, Dembski M, Weng Z, Deng N, Shyjan AW, Gimeno CJ, Iris R, Ellis SJ, Woolf EA, and Tartaglia LA. Cloning and characterization of an uncoupling protein homolog. A potential molecular mediator of human thermogenesis. *Diabetes* 46: 900–906, 1997.
- Gong D-W, He Y, Karas M, and Reitman M. Uncoupling protein-3 is a mediator of thermogenesis regulated by thyroid hormone,  $\beta_3$ -adrenergic agonists, and leptin. *J Biol Chem* 272: 24129–24132, 1997.
- Harper M-E and Brand MD. The quantitative contributions of mitochondrial proton leak and ATP turnover reactions to the changed respiration rates of hepatocytes from rats of different thyroid status. *J Biol Chem* 268: 14850–14860, 1993.
- Heaton GM, Wagenvoort RJ, Kemp A Jr, and Nicholls DG. Brown-adipose-tissue mitochondria: photoaffinity labeling of the regulatory site of energy dissipation. *Eur J Biochem* 82: 515–521, 1978.
- Hwang C-S, and Lane MD. Up-regulation of uncoupling protein-3 by fatty acid in C2C12 myotubes. *Biochem Biophys Res Commun* 258: 464–469, 1999.
- Jekabsons MB, Gregoire FM, Schonfeld-Warden NA, Warden CH, and Horwitz BA.  $T_3$  stimulates resting metabolism and UCP-2 and UCP-3 mRNA but not nonphosphorylating mitochondrial respiration in mice. *Am J Physiol Endocrinol Metab* 277: E380–E389, 1999.
- Kelly LJ, Vicario PP, Thompson GM, Candelore MR, Doebber TW, Ventre J, Wu MS, Meurer R, Forrest MJ, Conner MW, Cascieri MA, and Moller DE. Peroxisome proliferator-activated receptors  $\gamma$  and  $\alpha$  mediate *in vivo* regulation of uncoupling protein (UCP-1, UCP-2, UCP-3) gene expression. *Endocrinology* 139: 4920–4927, 1998.
- Kozak W, Conn CA, and Kluger MJ. Lipopolysaccharide induces fever and depresses locomotor activity in unrestrained mice. *Am J Physiol Regulatory Integrative Comp Physiol* 266: R125–R135, 1994.
- Lanni A, Beneduce L, Lombardi A, Moreno M, Boss O, Muzzin P, Giacobino J-P, and Goglia F. Expression of uncoupling protein-3 and mitochondrial activity in the transition from hypothyroid to hyperthyroid state in rat skeletal muscle. *FEBS Lett* 444: 250–254, 1999.
- Lanni A, De Felice M, Lombardi A, Moreno M, Fleury C, Ricquier D, and Goglia F. Induction of UCP2 mRNA by thyroid hormones in rat heart. *FEBS Lett* 418: 171–174, 1997.
- Larrouy D, Laharrague P, Carrera G, Viguerie-Bascands N, Levi-Meyrueis C, Fleury C, Pecqueur C, Nibelink M, André M, Casteilla L, and Ricquier D. Kupffer cells are a dominant site of uncoupling protein 2 expression in liver. *Biochem Biophys Res Commun* 235: 760–764, 1997.

27. **Mao W, Yu XX, Zhong A, Li W, Brush J, Sherwood SW, Adams SH, and Pan G.** UCP4, a novel brain-specific mitochondrial protein that reduces membrane potential in mammalian cells. *FEBS Lett* 443: 326–330, 1999.
28. **Marsh CB and Wewers MD.** The pathogenesis of sepsis. Factors that modulate the response to gram-negative bacterial infection. *Clin Chest Med* 17: 183–197, 1996.
29. **Masaki T, Yoshimatsu H, Kakuma T, Hidaka S, Kurokawa M, and Sakata T.** Enhanced expression of uncoupling protein 2 gene in rat white adipose tissue and skeletal muscle following chronic treatment with thyroid hormone. *FEBS Lett* 418: 323–326, 1997.
30. **McKnight AJ, Macfarlane AJ, Dri P, Turley L, Willis AC, and Gordon S.** Molecular cloning of F4/80, a murine macrophage-restricted cell surface glycoprotein with homology to the G-protein-linked transmembrane 7 hormone receptor family. *J Biol Chem* 271: 486–489, 1996.
31. **Millet L, Vidal H, Andreelli F, Larrouy D, Ricquier D, Laville M, and Langin D.** Increased uncoupling protein-2 and -3 mRNA expression during fasting in obese and lean humans. *J Clin Invest* 100: 2665–2669, 1997.
32. **Millet L, Vidal H, Larrouy D, Andreelli F, Laville M, and Langin D.** mRNA expression of the long and short forms of uncoupling protein-3 in obese and lean humans. *Diabetologia* 41: 829–832, 1998.
- 32a. **Porter RK, Joyce OJP, Farmer MK, Heneghan R, Tipton KF, Andrews JF, McBennett SM, Lund MD, Jensen CH, and Melia HP.** Indirect measurement of mitochondrial proton leak and its application. *Int J Obes* 23 (Suppl 6): S12–S18, 1999.
33. **Prashker D and Wardlaw AC.** Temperature responses of mice to *Escherichia coli* endotoxin. *Br J Exp Pathol* 52: 36–46, 1971.
34. **Puigserver P, Wu Z, Park CW, Graves R, Wright M, and Spiegelman BM.** A cold-inducible coactivator of nuclear receptors linked to adaptive thermogenesis. *Cell* 92: 829–839, 1998.
35. **Reynafarje B, Costa LE, and Lehninger AL.** O<sub>2</sub> solubility in aqueous media determined by a kinetic method. *Anal Biochem* 145: 406–418, 1985.
36. **Richter C, Schweizer M, and Ghafourifar P.** Mitochondria, nitric oxide, and peroxynitrite. *Methods Enzymol* 301: 381–393, 1999.
37. **Rolfe DFS, Hulbert AJ, and Brand MD.** Characteristics of mitochondrial proton leak and control of oxidative phosphorylation in the major oxygen-consuming tissues of the rat. *Biochim Biophys Acta* 1118: 405–416, 1994.
38. **Samec S, Seydoux J, and Dulloo AG.** Role of UCP homologues in skeletal muscles or brown adipose tissue: mediators of thermogenesis or regulators of lipids as fuel substrate? *FASEB J* 12: 715–724, 1998.
39. **Samec S, Seydoux J, and Dulloo AG.** Post-starvation gene expression of skeletal muscle uncoupling protein 2 and uncoupling protein 3 in response to dietary fat levels and fatty acid composition. *Diabetes* 48: 436–441, 1999.
40. **Sanchis D, Fleury C, Chomiki N, Goubern M, Huang Q, Neverova M, Grégoire F, Easlick J, Raimbault S, Clévi-Meyruies Miroux B, Collins S, Seldin M, Richard D, Warden C, Bouillaud F, and Ricquier D.** BMCP1, a novel mitochondrial carrier with high expression in the central nervous system of humans and rodents, and respiration uncoupling activity in recombinant yeast. *J Biol Chem* 273: 34611–34615, 1998.
41. **Shiomi M, Wakabayashi Y, Sano T, Shinoda Y, Nimura Y, Ishimura Y, and Suematsu M.** Nitric oxide suppression reversibly attenuates mitochondrial dysfunction and cholestasis in endotoxemic rat liver. *Hepatology* 27: 108–115, 1998.
42. **Vidal-Puig A, Solanes G, Grujic D, Flier JS, and Lowell BB.** UCP3: an uncoupling protein homologue expressed preferentially and abundantly in skeletal muscle and brown adipose tissue. *Biochem Biophys Res Commun* 235: 79–82, 1997.
43. **Wang H, Bloom O, Zhang M, Vishnubhakat JM, Ombrellino M, Che J, Frazier A, Yang H, Ivanova S, Borovikova L, Manogue KR, Faist E, Abraham E, Andersson J, Andersson U, Molina PE, Abumrad NN, Sama A, and Tracey KJ.** HMG-1 as a late mediator of endotoxin lethality in mice. *Science* 285: 248–251, 1999.
44. **Weigle DS, Selfridge LE, Schwartz MW, Seeley RJ, Cummings DE, Havel PJ, Kuijper JL, and BeltrandelRio H.** Elevated free fatty acids induce uncoupling protein 3 expression in muscle. A potential explanation for the effect of fasting. *Diabetes* 47: 398–302, 1998.
45. **Wu Z, Puigserver P, Andersson U, Zhang C, Adelmant G, Mootha V, Troy A, Cinti S, Lowell B, Scarpulla RC, and Spiegelman BM.** Mechanisms controlling mitochondrial biogenesis and respiration through the thermogenic coactivator PGC-1. *Cell* 98: 115–124, 1999.
46. **Yu XX, Mao W, Zhong A, Schow P, Brush J, Sherwood SW, Adams SH, and Pan G.** Characterization of novel UCP5/BMCP1 isoforms and differential regulation of UCP4 and UCP5 expression through dietary or temperature manipulation. *FASEB J*. In press.
47. **Zanetti G, Heumann D, Gérain J, Kohler J, Abbet P, Baras C, Lucas R, Glauser M-P, and Baumgartner J-D.** Cytokine production after intravenous or peritoneal gram-negative bacterial challenge in mice. *J Immunol* 148: 1890–1897, 1992.